MECSOL 2022 - Proceedings of the 8th International Symposium on Solid Mechanics
M.L. Bittencourt, J. Labaki, L.C.M. Vieira Jr. and E. Mesquita (Editors), Campinas SP, Brazil, October 17th to 19th, 2022

Variation of porosity in periodic micro-perforated chamber mufflers using spectral transfer matrix method

Wanderson Vinicius de O. Monteiro[1], Cássio Bruno F. Gomes[1] , Adriano M. Goto[2], Edilson D. Nóbrega[1] and José Maria C. Dos Santos[2]

[1] Federal University of Maranhão (UFMA)
[2] University of Campinas (UNICAMP)

Abstract. Micro-perforated chamber mufflers cause a reduction in the sound level of a system due to high acoustic resistance, and low mass reactance caused for its micro-perforations, making it an effective sound absorber. When arranged periodically it becomes more efficient. Transmission loss is related to the loss of sound waves transmission inside the silencer, and in a periodic acoustic device. For certain frequency bands, it can produce Bragg effect and local resonance, which generates bandgaps (stop band) where the waves can not propagate. These bands can be identified by calculating the dispersion curves, which can be obtained applying the Floquet-Bloch theorem. Here it is obtained using the Spectral Transfer Matrix method applied to a micro-perforated chamber muffler. This work analyzes the variation of porosity in a three-cell periodic micro-perforated chamber muffler. The sound pressure level and the transmission loss are also calculated and presented. It is observed that the transmission loss is not proportional to the amount of micro holes, showing the requirement to study porosity in the muffler's design. The diameter ratio directly influences the transmission loss, where the best value is obtained for a 0.8 mm micro hole diameter.
Keywords: Micro-perforated chamber muffler, Transmission Loss, Spectral Transfer Matrix, Floquet-Bloch theorem, Wave propagation

INTRODUCTION

Through the study of acoustics, it is possible to develop the noise control generated by machines, equipment or similar devices by using expansion chamber muffler. Maa (1987) was the pioneer in the study of micro-perforated panel (MPP). It is an acoustic device made with a thin plate with small holes punched in it, backed with a rigid wall. Due to the sub-millimeter dimension of the holes, the MPP has a high acoustic resistance and low mass reactance, making the acoustic system an efficient sound absorber.

MPP's have the potential to replace more traditional sound absorption materials as they avoid problems of bacterial contamination and discharge of small particles. The sound energy loss occurs from the viscous dissipation of air, oscillating in its holes. Due to its sound absorption performance, it can be selected for buildings and residences (Xu et al., 2020).

Micro-perforated chamber muffler (MPCM) is composed by a duct with small holes punched in it, surrounded by an expansion chamber. The mainly methods applied in MPCM studies are the Finite Element Method (FEM), Boundary Element Method (BEM) and Spectral Transfer Matrix (STM).

Some researches on MPCM includes the works of Tan and Mak (2013) and Alisah et al. (2021) who used simulations by BEM and experimental test to investigate the sound transmission loss (TL) of MPCM by changing the the expansion chamber length and the hole diameter. By using experimental test and simulations by FEM, Xiang et al. (2013) analyzed the effect of changing the micro-perforated tube length on the TL. Also, they related it to rotating machines for noise control. Shi and Mark (2017) investigated, analytically with experimental validation, periodic arrangements of MPCM by changing geometric parameters, in order to observe the influences on the TL. Chen et al. (2020) proposed a serial-parallel MPCM model, using the FEM and experimental validation, to reduce the intake noise of a vehicle engine under accelerated working conditions.

In this work, the dispersion diagram, the sound pressure level (SPL) and sound transmission loss (TL) of periodic micro-perforated chamber silencer are calculated using the STM method for different porosities.

SPECTRAL TRANSFER MATRIX

Acoustic duct formulation

According to Kinsler et al. (1998), for a 1-D acoustic duct the non-dissipative wave equation can be written in frequency domain as:

$$\frac{d^2p}{dx^2} + k^2 p(x) = 0, \tag{1}$$

where p the acoustic pressure, x is the space, t the time, $k = \omega/c_0$ is the wave number with c_0 as the sound speed in the air and ω is the circular frequency. The solution of Eq. (1) can be written as:

$$p(x) = Ae^{j(\omega t - kx)} + Be^{j(\omega t + kx)}. \tag{2}$$

The constants A and B are determined by boundary conditions and j is the imaginary unit. From Eq. (2), the mass velocity is obtained as:

$$v(x) = -\frac{1}{Y}(Ae^{-j(\omega t - kx)} - Be^{j(\omega t + kx)}), \tag{3}$$

where $Y = c_0/S_d$ is the characteristic impedance with S_d as the duct cross-sectional area. From Eqs. (2) and (3), the input and output relationship of mass velocity and acoustic pressure of a duct with length L can be obtained as (Munjal,1987):

$$\begin{Bmatrix} v_0 \\ p_0 \end{Bmatrix} = \underbrace{\begin{bmatrix} \cos(kL) & jY\sin(kL) \\ \frac{j}{Y}\sin(kL) & \cos(kL) \end{bmatrix}}_{\mathbf{T_d}} \begin{Bmatrix} v_L \\ p_L \end{Bmatrix}, \tag{4}$$

where $\mathbf{T_d}$ is the transfer matrix of a duct, $\{v_0\ p_0\}^T$ and $\{v_L\ p_L\}^T$ are the inlet and outlet vectors, respectively, of mass velocity and acoustic pressure.

Micro-perforated chamber muffler formulation

Figure 1 shows the MPCM analyzed in this study, where Fig. 1a shows the internal duct with the micro holes, and Fig. 1b shows the assemblage of internal duct with the expansion chamber.

(a) **Internal duct.** (b) **Assemblage of internal duct with chamber.**

Figure 1 – Micro-perforated chamber muffler.

The relationship between acoustic pressure and mass velocity is given by (Kinsler et al., 1998):

$$\frac{dp}{dx} = -jkYv. \tag{5}$$

Assuming plane wave propagation inside the perforated duct and chamber, the behavior of the system can be represented as in Fig. 2.

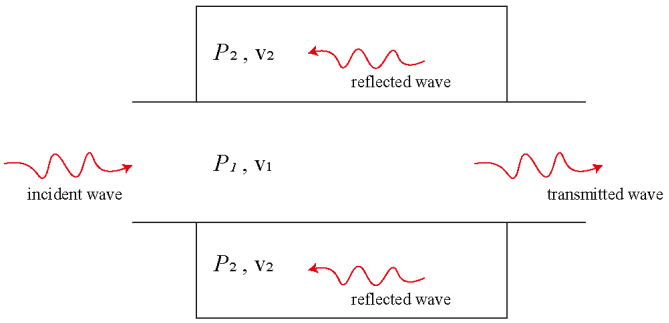

Figure 2 – Wave propagation in a micro-perforated chamber muffler.

Note that the mass velocity and acoustic pressure in the perforated duct and expansion chamber are different, thus the system govern equations are given by (Selamet et al., 2003):

$$\begin{aligned}\frac{d^2p_1}{dx^2}+(k^2-j\frac{4}{D_0}\frac{k}{z})p_1+j\frac{4}{D_0}\frac{k}{z}p_2=0\\ \frac{d^2p_2}{dx^2}+j\frac{4D_0}{D^2-D_0^2}\frac{k}{z}p_1+(k^2-j\frac{4D_0}{D^2-D_0^2}\frac{k}{z})p_2=0,\end{aligned} \tag{6}$$

where D and D_0 are the micro-perforated duct and the expansion chamber diameters, respectively. The micro hole specific acoustic impedance is give by (Maa, 1975):

$$z=\frac{32\eta_{air}}{\sigma\rho c}\frac{t_h}{d_h^2}\left[\sqrt{1+\frac{K^2}{32}}+\frac{\sqrt{2}}{32}K\frac{d_h}{t_h}\right]+j\frac{\omega t_h}{\sigma c}\left[1+\frac{1}{\sqrt{9+\frac{K^2}{2}}}+0.85\frac{d_h}{t_h}\right], \tag{7}$$

where $K=d_h\sqrt{\omega\rho/4\eta_{air}}$ with η_{air} as the air viscosity, ρ is the air mass density, d_h is the micro hole diameter, and t_h is the wall thickness of the micro-perforated. Also, $\sigma=N_fA_f/A_L$, where N_f is the number of holes, A_f is the area of holes, and A_L is the perforated area of the duct. From Eqs. (5) and (6), the state-space formulation is obtained as:

$$\frac{d}{dx}\begin{Bmatrix}p_1\\-v_1\\p_2\\-v_2\end{Bmatrix}=\underbrace{\begin{bmatrix}0 & jkY_1 & 0 & 0\\ \frac{4}{D_0zY_1}+j\frac{k}{Y_1} & 0 & -\frac{4}{D_0zY_1} & 0\\ 0 & 0 & 0 & jkY_2\\ -\frac{4D_0}{(D^2-D_0^2)zY_2} & 0 & \frac{4D_0}{(D^2-D_0^2)zY_2} & 0\end{bmatrix}}_{\mathbf{T}_G}\begin{Bmatrix}p_1\\-v_1\\p_2\\-v_2\end{Bmatrix}, \tag{8}$$

where $Y_i=c_0/S_i$ with S_i $i=1,2$ as the cross-section areas of micro-perforated duct and chamber, respectively.

The transfer matrix can be obtained numerically. However, it gives a 4×4 matrix. To reduce to an 2×2 matrix, it was assumed $v_2(0)=0$ and $v_2(L)=0$. Thus, the transfer matrix for the micro-perforated chamber muffler can be obtained as:

$$\mathbf{T}_m=\begin{bmatrix}T_{G_{11}}-\frac{T_{G_{13}}T_{G_{41}}}{T_{G_{43}}} & T_{G_{12}}-\frac{T_{G_{13}}T_{G_{42}}}{T_{G_{43}}}\\ T_{G_{21}}-\frac{T_{G_{23}}T_{G_{41}}}{T_{G_{43}}} & T_{G_{22}}-\frac{T_{G_{23}}T_{G_{42}}}{T_{G_{43}}}\end{bmatrix}, \tag{9}$$

where the terms $T_{G_{ij}}$ $i,j=1\cdots4$, are the terms of the 4×4 transfer matrix of Eq. (8).

The unit-cell transfer matrix of a periodic micro-perforated chamber mufflers is the combination of two ducts (inlet and outlet) with one micro-perforated duct and chamber transfer matrices, given by:

$$\mathbf{T}=\mathbf{T}_{d_i}\mathbf{T}_m\mathbf{T}_{d_o}. \tag{10}$$

Figure 3 shows a periodic arrangement of micro-perforated chamber mufflers.

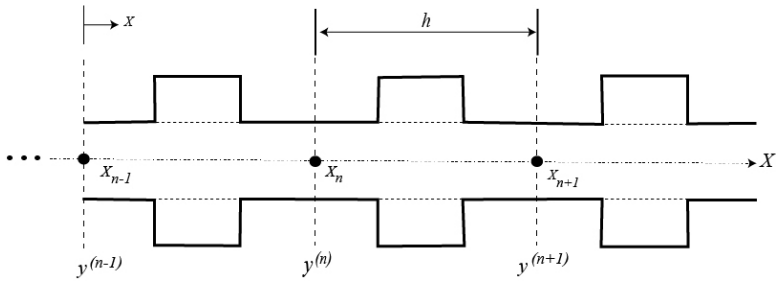

Figure 3 – Periodic micro-perforated chamber mufflers.

The transfer matrix relates the inputs from the right ($y_r^{(n)}$) to the output from the left ($y_l^{(n)}$), this is:

$$y_r^{(n)} = \mathbf{T} y_l^{(n)}. \tag{11}$$

Using the coupling relation, applying Floquet-Bloch theorem and disregarding the index, it is obtained:

$$\mathbf{T}y = e^{\mu}\mathbf{T}y, \tag{12}$$

which is an eigenproblem where e^{μ} is the eigenvalue and y is the eigenvector. Whence the attenuation constant is obtained as $\mu = -j \cdot k_B h$, where k_B is the Bloch wavenumber and h is the unite-cell length (duct inlet length + micro-perforated duct-chamber length + duct outlet length). In the case of plane wave propagation, sound pressure and mass velocity can be expressed as a function of incident and reflected wave amplitudes.

$$\begin{aligned} p_n(x) &= I_n e^{-jk(x-x_n)} + R_n e^{jk(x-x_n)}, \\ v_n(x) &= -\frac{1}{Y}(I_n e^{-jk(x-x_n)} - R_n e^{jk(x-x_n)}), \end{aligned} \tag{13}$$

where x_n represents the center of the uniform duct at the $n-th$ position, I_n and R_n are the incident and reflected wave amplitudes at the $n-th$ position of the periodic arrangement, respectively. Then, Eq. (13) can be written as:

$$y^n(x) = \begin{Bmatrix} p_n(x) \\ -v_n(x) \end{Bmatrix} = \underbrace{\begin{bmatrix} e^{-jk(x-x_n)} & e^{jk(x-x_n)} \\ \frac{e^{-jk(x-x_n)}}{Y} & -\frac{e^{jk(x-x_n)}}{Y} \end{bmatrix}}_{\mathbf{H}^{(n)}(x)} \underbrace{\begin{Bmatrix} I_n \\ R_n \end{Bmatrix}}_{C_n}. \tag{14}$$

Then, relating $\mathbf{C}_n$ and $\mathbf{C}_{n+1}$ through the interface coupling relationship:

$$\mathbf{C_{n+1}} = \underbrace{[\mathbf{H}^{(n+1)}(x_n+1)]^{-1}\mathbf{T}\mathbf{H}^n(x_n)}_{\mathbf{T}_p}\mathbf{C}_n. \tag{15}$$

The transfer matrix referring to the wave amplitudes is given by $\mathbf{T}_p$. The incident and reflected wave amplitudes can be obtained from the eigenvectors and eigenvalues of the matrix $\mathbf{T}_p$, as follows:

$$\begin{Bmatrix} I_1 \\ R_1 \end{Bmatrix} = a \begin{Bmatrix} \Phi_I^+ \\ \Phi_R^+ \end{Bmatrix} + \begin{Bmatrix} \Phi_I^- \\ \Phi_R^- \end{Bmatrix}, \tag{16}$$

$$\begin{Bmatrix} I_n \\ R_n \end{Bmatrix} = \mathbf{T}_p^n \begin{Bmatrix} I_1 \\ R_1 \end{Bmatrix} = a e^{\mu^+ n} \begin{Bmatrix} \Phi_I^+ \\ \Phi_R^+ \end{Bmatrix} + b e^{\mu^- n} \begin{Bmatrix} \Phi_I^- \\ \Phi_R^- \end{Bmatrix}, \tag{17}$$

where a and b are determined by the boundary conditions. Bloch waves can propagate in the positive $(+)$ and negative $(-)$ directions of the wave direction, what determines this direction is the ratio between the eigenvalues of the matrix $\mathbf{T}_p$.

Case $|\Phi_i/\Phi_R| > 1$, the displacement of the Bloch wave occurs in the positive direction, if $|\Phi_i/\Phi_R| < 1$ the displacement is in the negative direction.

The Transmission Loss (TL) is obtained as:

$$TL = 20\log\left(\frac{1}{a_t}\right), \tag{18}$$

where a_t is the sound power transmission coefficient, given by:

$$a_t^2 = \left|\frac{I_n}{I_1}\right|^2 = \left|\frac{ae^{\mu^+ n}\Phi_I^+ + be^{\mu^- n}\Phi_I^-}{a\Phi_I^+ + b\Phi_I^-}\right|^2. \tag{19}$$

To obtain the constants a and b, it is possible to consider the anechoic termination of the system, thus $R_n = 0$ and the coefficients are given by:

$$\frac{b}{a} = -\frac{e^{\mu^+ n}\Phi_R^+}{e^{\mu^- n}\Phi_R^-} \tag{20}$$

The forced response in a periodic structure of the micro-perforated chamber muffler can be obtained using the eigenvalues and eigenvectors obtained by the Floquet-Bloch theorem. Eigenvalues can be divided into two groups: $|e^{\mu_i}| \leq 1$, $i = 1,2,\ldots m$, where m represents the degrees of freedom, indicate the wave propagation to the right and $|e^{\mu_i}| \geq 1$, $i = 1,2,\ldots m$, indicate the wave propagation to the left. Then, the state vectors y^n can be expressed as (Silva and Arruda, 2014):

$$y^n = \sum_i^m e^{-jk_i L}\Phi_i y_i^n. \tag{21}$$

where $n = 1,2,3\ldots N_c$ and N_c represents quantity of unit cells of the periodic system. Considering a anechoic termination, from Eq. (13) it is obtained the input and output velocities.

$$v_1 = \frac{-I_1 + R_1}{Y}, \qquad v_N = -\frac{I_N}{Y}, \tag{22}$$

where I_1, R_1 and I_n can be obtained from Eqs. (16), (17) e 20, and q_1 and q_2 are the Bloch's wave numbers obtained from the transfer matrix of the cell.

$$\begin{aligned} I_1 &= \Phi_I^+ - \frac{\Phi_R^+\Phi_I^-}{\Phi_R^-}e^{-j(q_1-q_2)hN_c} \\ R_1 &= (1 - e^{-j(q_1-q_2)hN_c})\Phi_R^+ \qquad I_N = (\Phi_I^+ - \frac{\Phi_R^+\Phi_I^-}{\Phi_R^-})e^{-jq_1 hN_c}. \end{aligned} \tag{23}$$

NUMERICAL RESULTS

Table 1 shows the geometric and air properties of the micro-perforated chamber silencer. Although not shown here, numerical validation was performed comparing the TL's obtained by the STM and FEM (COMSOL).

Table 1 – Properties for the chamber muffler.

Property	Value
Density (kg·m^{-3})	1.204
Velocity (m·s^{-1})	343.3
Viscosity (Pa·s)	1.8x10^{-5}
Duct diameter (m)	75x10^{-3}
Duct length (m)	100x10^{-3}
Expansion chamber diameter (m)	150x10^{-3}
Expansion chamber length (m)	150x10^{-3}
Duct thickness (m)	3x10^{-3}
Diameter hole (m)	0.7x10^{-3}
Number of cell	3

Porosity Evaluation

For an MPCM with 400 holes, and considering the data in Tab. 1, Fig. 4 shows the dispersion diagram and sound pressure level (SPL), varying the frequency from 0 to 2000 Hz. The dispersion diagram has the positive and negative parts of the Bloch wavenumber as a function of the frequency. The highlighted region of the graph shows the bandgaps, region where the imaginary part of the Bloch wavenumber is different from zero, as the real part is different from zero or π, it means that the wave propagation still occurs, even though with a damping factor due to micro-perforations. The graph also shows the effect of local resonance near to 1200 Hz. In the SPL graph, it is possible to identify the attenuation caused by micro-perforations in the same frequency range where the bandgap occurs in the disperstion diagram (70 - 800 Hz). It also shows the highest attenuation values, showing that the micro-perforations act in the lower frequency regions, in addition to the attenuation caused by the local resonance effect.

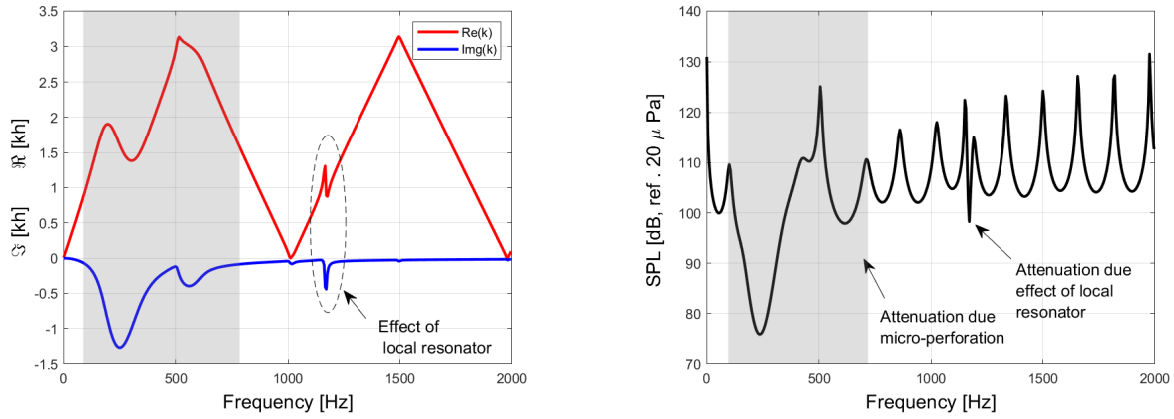

Figure 4 – Dispersion diagram and sound pressure level for a micro-perforated chamber muffler.

Figure 5 shows the loss of sound transmission in MPCM,where, as already shown in the SPL,the greatest attenuation occurs in the frequency range between 70 and 440 Hz,with a lower attenuation between 460 and 600 Hz,in addition to the attenuation caused by the local resonance effect at 1200 Hz. Attenuation are caused by the loss of sound energy due to viscous air dissipation oscillating in its perforations and by the Bragg effect.

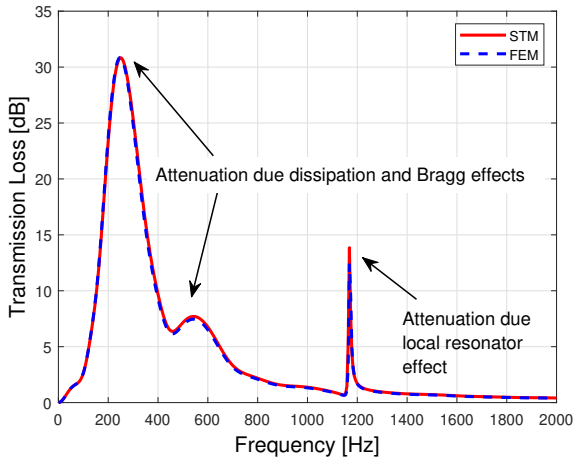

Figure 5 – Transmission loss curve for the micro-perforated chamber muffler.

Porosity is the ratio between the total area of the micro-perforations and the area of the micro-perforated duct,its main parameters are the number of holes, diameter of the micro-perforated, and the area of the micro-perforated duct. Fig. 6 shows the variation in the number of holes in an MPCM, whose properties are shown in Tab. 1, as a function of

frequency. The influence of porosity is shown by the TL magnitude. Note that with increasing porosity, the region of greatest attenuation goes from 400 Hz (as shown in Fig. 5) to a range of 600 - 1000 Hz. It is verified that the highest values and width of the TL occur between 1400 and 1800 holes, around 65 dB. From 1800 holes there is a gradual loss of the TL magnitude. Note also that for frequencies above 1000 Hz, this MPCM configuration is no longer effective for noise control. Therefore, in the MPCM design, a study should be carried out on the ideal amount of micro-perforations to generate the highest attenuation values, which is not necessarily the largest possible number of holes.

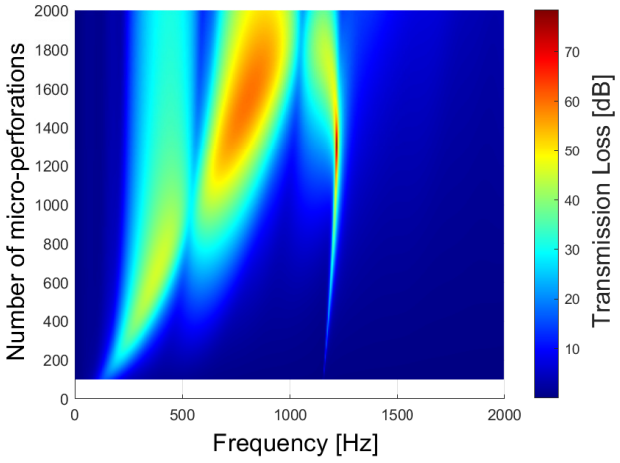

Figure 6 – Influence of number of holes in the Transmission Loss for the MPCM.

Figure 7 shows the ratio between the diameters of the expansion chamber and the micro-perforated duct with 1500 holes, quantity with the best attenuation obtained previously. The porosity is inversely proportional to the diameter of the micro-perforation. It is observed that the largest attenuation bands are located at low frequencies, as well as for smaller diameter ratios. The smaller the relationship between the diameters, the greater the attenuation values are obtained, a result also observed by Alisah et al (2021).

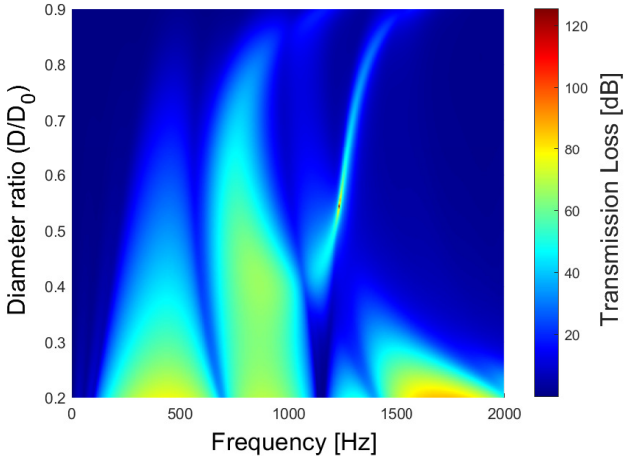

Figure 7 – Influence of diameter ratio $(\mathbf{D}/\mathbf{D_0})$ the Transmission Loss for the MPCM.

Figure 8 shows TL values for micro-perforation diameter variation in MPCM. The results indicate that the highest values and ranges of attenuation in the TL are for a diameter equal to 0.8 mm, in the frequency range from 600 to 900 Hz. Note that for very small diameter ratios, the frequency bandwidths of attenuation become larger, although they are not very high.

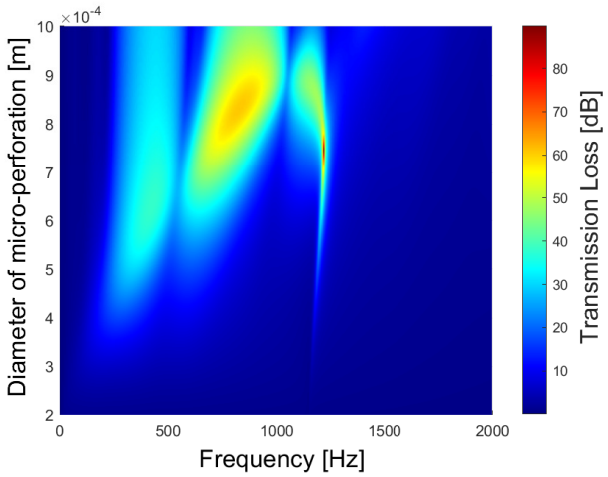

Figure 8 – Influence of diameter micro-perforation on MPCM.

CONCLUSIONS

The present work investigated the effect of porosity variation in a micro-perforated chamber muffler through the spectral transfer matrix (STM) method. From the analytical modeling, the dispersion diagram was obtained that detail the bandgaps regions and the sound pressure level (SPL), which is a forced response of the system, in addition to the sound transmission loss (TL) of the MPCM.

Using the SPL response and the dispersion diagram, it was possible to visualize the bandgaps and attenuation regions, which occur at low frequencies and are caused by micro-perforations. In the TL response, these attenuation values occur in the same frequency range as the bandgaps in the dispersion diagram, and are caused by the loss of sound energy due to viscous air dissipation in the micro-perforations, in addition to the destructive Bragg effect.

In the porosity analysis, it was observed that with the increase in the number of micro-perforations, the sound transmission loss increases up to a given limit of holes, from where it starts to decay considerably. In the MPCM design, there must be a study of the number of ideal holes to obtain the highest attenuation values. Regarding the diameter of the micro-perforated duct, the smaller its diameter in relation to the expansion chamber, the greater the values are obtained in the attenuation of the waves. Values close to 0.8 mm for the diameter of the micro-perforation indicated the best results for noise control.

ACKNOWLEDGMENTS

The authors are grateful to the Brazilian research funding agencies FAPEMA (Grant No.BM-07223/22), CAPES,CNPq (Grant No. 317436/2021) and FAPESP (Grant No. 16794-2/2019; Grant No. 15894-0/2018) for the financial support.

REFERENCES

ALISAH, M. et al, 2021, ”Acoustic attenuation performance analysis and optimisation of expansion chamber coupled micro-perforated cylindrical panel using response surface method. Archives of Acoustics”, v. 46, n. 3.

CHEN, W.; LU, C.; LIU, Z, 2020, ”Optimal design of a 3d printed composite micro-perforated silencer for engine intake noise control”. IOP Conference Series: Materials Science and Engineering, v. 774, p. 012125, 03.

KINSLER Austin r. Frey, A. B. C. J. V. S. L. E, 1998, ”Fundamentals of acoustics”. 4. ed. [S.l.]: Wiley. ISBN 9780471847892,0471847895.

MAA, D. Y, 1975, ”Theory and design of microperforated panel sound-absorbing constructions”.

MUNJAL, M.L., 1987. ”Acoustics of Ducts and Mufflers With Application to Exhaust and Ventilation System Design”. Wiley, 1st edition. ISBN 0471847380,9780471847380

SELAMET, A.; LEE, I.; HUFF, N,2003, ”Acoustic attenuation of hybrid silencers”. Journal of Sound and Vibration, v. 262, n. 3, p. 509–527. ISSN 0022-460X. India-USA.Symposium on Emerging Trends in Vibration and Noise Engineering

SHI, X.; MAK, C.-M, 2017, "Sound attenuation of a periodic array of micro-perforated tube mufflers. Applied Acoustics", v. 115, p. 15–22. ISSN 0003-682X

SILVA, P., Mencik, J.M. and Arruda, J., 2014. "On the forced harmonic response of coupled systems via a wfe-based super-element approach".In Proceedings of ISMA, pages 1–13

TAN, W.; RIPIN, Z. mohd, 2013, "Analysis of exhaust muffler with micro-perforated panel". Journal of Vibroengineering, v. 15, p. 558–573, 06.

XIANG, L. et al, 2013, "Study of micro-perforated tube mufflers with adjustable transmission loss". The Journal of the Acoustical Society of America, v. 134, p. 4217, 11 .

XU, Z. et al, 2020, "Sound absorption theory for micro-perforated panel with petal-shaped perforations (L)". The Journal of the Acoustical Society of America, v. 148, p. 18–24, 07.

RESPONSIBILITY NOTICE

The authors are the only parties responsible for the printed material included in this paper.